Nuclear Engineering and Technology 49 (2017) 663–667

Contents lists available at ScienceDirect

Nuclear Engineering and Technology

journal homepage: www.elsevier.com/locate/net

Original Article

On the effect of temperature on the threshold stress intensity factor of delayed hydride cracking in light water reactor fuel cladding

Anna-Maria Alvarez Holston*, Johan Stjärnsäter

Studsvik Nuclear AB, Nyköping 61182, Sweden

ARTICLE INFO

Article history:
Received 12 April 2017
Accepted 14 April 2017
Available online 20 April 2017

Keywords:
Delayed Hydride Cracking
Fuel Cladding Integrity
Pin Loading Testing
Threshold Stress Intensity Factor
Zry-4

ABSTRACT

Delayed hydride cracking (DHC) was first observed in pressure tubes in Canadian CANDU reactors. In light water reactors, DHC was not observed until the late 1990s in high-burnup boiling water reactor (BWR) fuel cladding. In recent years, the focus on DHC has resurfaced in light of the increased interest in the cladding integrity during interim conditions. In principle, all spent fuel in the wet pools has sufficient hydrogen content for DHC to operate below 300°C. It is therefore of importance to establish the critical parameters for DHC to operate. This work studies the threshold stress intensity factor (K_{IH}) to initiate DHC as a function of temperature in Zry-4 for temperatures between 227°C and 315°C. The experimental technique used in this study was the pin-loading testing technique. To determine the K_{IH}, an unloading method was used where the load was successively reduced in a stepwise manner until no cracking was observed during 24 hours. The results showed that there was moderate temperature behavior at lower temperatures. Around 300°C, there was a sharp increase in K_{IH} indicating the upper temperature limit for DHC. The value for K_{IH} at 227°C was determined to be 2.6 ± 0.3 MPa $\sqrt{m}$.

1. Introduction

Fuel cladding constitutes the first barrier to prevent the release of radioactive fission products and transuranium elements. Maintaining the cladding integrity is therefore, a fundamental concern for reactor safety. Until recently, the majority of the research on fuel cladding integrity has been focused on failures occurring during operation. However, as the wet pools at the reactor sites are filling up and no final disposal is in place, more emphasis is put into understanding the fuel behavior during interim and dry storage conditions.

The temperature and, consequently, the internal pressure P are highest at the start of dry storage. The US Nuclear Regulatory Commission requires cladding temperature not to exceed 400°C and cladding hoop stress to be <90 MPa. Thereafter, the fuel rods will slowly cool down, and after 40 years the cladding would have reached a temperature of approximately 200°C. At the highest temperature, the dominant deformation mechanism is creep; meanwhile, hydride-induced failures are one of the main concerns at temperatures below 300°C. Two types of hydride-induced failure mechanisms have been observed in zirconium alloys: one that acts on the macroscopic scale and the other that acts locally, in front of a stress concentrator. The first one is the classical hydride embrittlement that occurs instantaneously on a macroscopic level once the stress exceeds the fracture stress of a highly hydrided component [1–4]. The second mechanism, delayed hydride cracking (DHC), is a time-dependent mechanism that acts on a local level. It operates at much lower macroscopic hydrogen and stress levels than the classical hydride embrittlement. This study will focus on the latter failure mechanism and the threshold for temperatures below operating temperatures.

1.1. Delayed hydride cracking in zirconium alloys

Delayed hydride cracking (DHC) was first observed in the late 1960s to early 1970s in pressure tubes made of the Zr–2.5 wt% Nb alloy in Canadian CANDU reactors [5]. In the classical DHC model shown schematically in Fig. 1, hydrogen diffuses to stress concentrators or flaws, where brittle hydrides precipitate once the local solubility limit is exceeded [6, 7]. The density of hydrides increases as more hydrogen arrives, until the hydrided zone in front of the flaw cannot withstand the local tensile stress and fractures. The process then repeats leading to stepwise crack propagation.

* Corresponding author.
E-mail address: anna-maria.alvarez@studsvik.se (A.-M. Alvarez Holston).

http://dx.doi.org/10.1016/j.net.2017.04.002

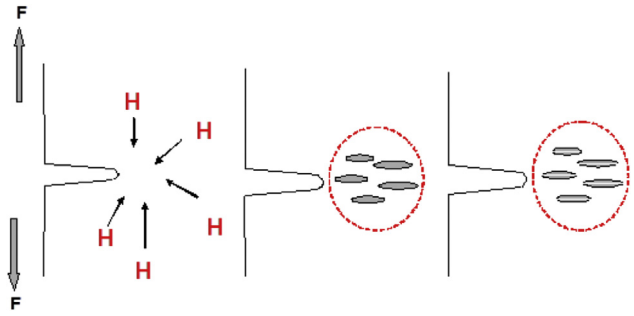

Fig. 1. Schematic illustration of DHC crack propagation. When an external load is applied, hydrogen in solid solution diffuses to stress concentrators, where hydrides precipitates locally after the solid solubility limit is exceeded. Hydride formation reduces the fracture strength in the zone in front of the crack tip, which fractures under the tensile load. DHC, delayed hydride cracking.

The critical parameters for DHC to occur have been studied extensively, especially for Zr pressure tubes in CANDU reactors and, more recently, also for fuel cladding in light water reactors. In Table 1, critical parameters for DHC and experimentally observed values are listed.

All the critical parameters have to be fulfilled simultaneously for DHC to occur. In most boiling water reactor (BWR) fuel claddings the three first requirements in Table 1 are fulfilled. Even so, no primary cladding failures due to DHC was reported until the so-called axial splits were observed during ramp tests of high-burnup light water reactor cladding. (Cladding defects in zirconium alloy cladding sometimes have the shape of long axial cracks or "splits." These long cracks have mainly been observed to occur in power ramp tests of high-burnup BWR fuel, but in some cases they also occur as secondary failures during operation. One often proposed mechanism responsible for the propagation of axial splits is hydrogen-induced cracking.) One explanation for the absence of DHC failures in low to medium burnup fuel cladding is the lack of any obvious stress concentrators. No internal stress is built up during production of the cladding tubes, as was the case for the early CANDU pressure tubes. Furthermore, pellet expansion is low at low burnup levels, limiting the cladding hoop stress. After extended periods of time in the reactor, however, the build-up of surface oxide and hydride rims will change the local stress distribution and incipient cracks may form in the oxide, hydride dense rim, or possibly in radial hydrides, which serve as potential initiation sites for DHC. Simultaneously, pellet expansion increases at higher burnup, increasing the stress exerted on the cladding. The increase in hoop stress in combination with incipient cracks may eventually cause the stress intensity in front of incipient cracks to exceed the threshold for DHC. Since all critical parameters except the critical stress intensity are fulfilled for most medium- and high-burnup rods in operation of a light water reactor, as well as for the rods during back end handling, it is of great importance to examine the threshold stress intensity factor (K_{IH}) more carefully so as to narrow the wide scatter in the results. As seen from the table, the value of K_{IH} in the literature varies from 4 MPa $\sqrt{m}$ to 12 MPa $\sqrt{m}$. An estimate of the critical depth of a flaw based on the value of K_{IH} can be derived from the following expression [22]:

$$a = (K_{IH}/\sigma)^2 \cdot Q/1.2\pi \quad (1)$$

where σ is the applied stress and Q is a geometry factor, which is 1.5 for elliptical flaws and 1 for long flaws.

Assuming a long flaw and the US Nuclear Regulatory Commission limit of 90 MPa during dry storage [23], the critical incipient flaw depth would be 0.52 mm for $K_{IH} = 4$ MPa $\sqrt{m}$ and 4.7 mm for $K_{IH} = 12$ MPa $\sqrt{m}$.

In order to determine whether DHC is a concern or not for a certain fuel cladding during the back end handling, it is important that the critical crack length for DHC is determined more precisely.

The objective of this work is to determine K_{IH} as a function of temperature with as low scatter as possible in the data, so that the critical crack length to initiate DHC at a certain internal pressure can be determined as accurately as possible.

2. Experimental details

2.1. Sample preparation

The material used in this study consists of pressure water reactor stress relief annealed Zry-4 cladding tubes with the dimensions, final heat treatment, chemical composition, and mechanical properties as shown in Table 2.

Cladding pieces with a length of 220 mm were electrolytically hydrogen charged to produce a hydride layer of about 10 μm at the outer surface of the tube. The hydride pieces were thereafter heat treated at 375°C for 24 hours to obtain an average hydrogen concentration of about 140 weight ppm (wppm) H. Cross sections were taken in order to confirm that the hydrides were circumferential

Table 2
Material data of SRA Zry-4 cladding used in this study.

Data	Value
Dimensions of each rod	OD = 9.5 mm, WT = 0.57
Final annealing conditions	5 hr at 480°C
Vendor lot #	407130
$Rp^{0.2}$ at RT	600 MPa
Rm at RT	815 MPa
A50mm at RT	18%
Chemical composition	
Sn	1.29-1.33%
Fe	0.21-0.22%
Cr	0.10-0.11%
O	1,270–1,351 ppm
Si	93-97 ppm
C	148-153 ppm

OD, outer diameter; RT = room temperature; SRA, stress relief annealed; WT, wall thickness.

Table 1
Values of the critical parameters for DHC, as observed in out-of-pile tests.

Critical parameter	Value	References	Comment
Minimum hydrogen concentration C_H (wppm)	$C_{TSSP} < C_{Hcrit} < C_{TSSD}$	[8–11]	$T = 300$°C, C_H (DHC) ~ 85 wppm H $T = 385$°C, C_H (DHC) ~ 210 wppm H
Maximum temperature T_{max} (°C)	350–385°C (high BU fuel cladding)	[12]	The upper temperature limit for DHC is dependent on burnup level
Sufficient time for through wall cracking or minimum crack velocity V_{DHC} (m/sec)	$V_{DCH} = 2 \times 10^{-7} - 5 \times 10^{-7}$ at 300°C	[13,14]	20–50 min for through wall failure at 300°C and wall thickness of 600 μm
Stress intensity above threshold, K_{IH} (MPa $\sqrt{m}$)	4–12	[15–21]	—

BU, burnup; C_{TSSP}, terminal solid solubility limit for hydride precipitation; C_{TSSD}, terminal solid solubility limit for hydride dissolution; C_{Hcrit}, critical hydrogen concentration for DHC to operate; DHC, delayed hydride cracking; K_{IH}, threshold stress intensity factor; wppm, weight parts per million.

and homogeneously distributed. The hydride area fraction was determined by image analysis using the backscattered electron imaging mode. When evaluating the hydride area fraction, it was assumed that (1) the amount of hydrogen in solid solution is negligible in comparison with the amount in the hydrides and (2) the hydrides are in δ-phase, with $ZrH_{1.62}$ corresponding to 62 atomic% hydrogen. The hydrogen fraction in wppm is calculated using the following formula:

$$W_H = W_\delta \cdot F \cdot \rho_\delta / (\rho_{Zr} \cdot (1 - F) + \rho_\delta \cdot F) \quad (2)$$

where,

W_H = wppm hydrogen
W_δ = wppm hydrogen in δ-phase hydride
F = measured area fraction
ρ_δ = density of the δ-phase hydride (5.65 g/cm^3)
ρ_{Zr} = density of the α-phase metal (6.54 g/cm^3)

2.2. Test method

A pin-loading tension (PLT) technique, developed to study DHC [20], was used in the tests. Configurations of the PLT specimen and fixture are shown in Fig. 2. The PLT fixture consists of two halves, which when placed together form a cylindrical holder. The cylindrical holder has a diameter, which allows it to be inserted into the tubular PLT specimen. The fixture halves are loaded in tension through pins at A and rotated about pin B in the figure.

Prior to starting the test, the specimen was fatigue pre-cracked to produce a sharp crack of about 1.5 mm in front of the machined notch C. During the DHC test, the specimen was heated to 385°C for 60 minutes to dissolve most of the hydrides, with a low load on the specimen. The sample was then cooled with no undercooling to the test temperature. After 30 minutes, the sample was loaded to a maximum K_I of 15 MPa $\sqrt{m}$, where the load was held constant until the crack started to propagate. During the test, crack advance was measured continuously with the direct current potential drop technique. Once the crack had grown a certain length, the load was reduced and the process repeated until no cracking was detected for 24 hours. This value of K_I represents the threshold value K_{IH}.

3. Results

A typical test curve from the DHC PLT tests is shown in Fig. 3. One can notice that the time to reach a certain crack length increases as the load decreases until the crack arrests for more than 24 hours. After the test was complete, the load was removed and the sample was cooled to room temperature. The specimen was then postfatigued in air at room temperature and broken open in two pieces. Fig. 4 shows a typical sample after it has been broken up. Since the fractography differs under different loading conditions, one can distinguish the different zones using a light microscope. The area identified as crack propagation by DHC was examined using a scanning electron microscope at higher magnification. Fractographic examination revealed that the fracture surface is dominated by quasi-cleavage surfaces parallel to the macroplane of the fracture surface plane. This type of fracture appearance in Zr cladding is characteristic of a DHC failure, where the failure occurs by fracture of brittle hydrides that are formed in front of the crack tip. Two mating surfaces normally match perfectly, and the plastic ridges are formed only on the steep sides connecting valleys with hills. As seen in Fig. 4, the two parallel cracks starting at the two opposite notches are similar, indicating that the variation in the initial notch and fatigue cracks is small and the sample is well aligned.

Table 3 shows a summary of all test data and measurements after the test.

K_I was calculated from the following equation:

$$K_I = \left[P \Big/ \left(2t\sqrt{W}\right)\right] f(a/W) \quad (3)$$

where

P = load applied to specimen (N)
t = wall thickness of the cladding (m)
W = effective width of the specimen (m), being the distance from the load line to axis of rotation
a = effective crack length (m), being the distance from the load line to the crack tip

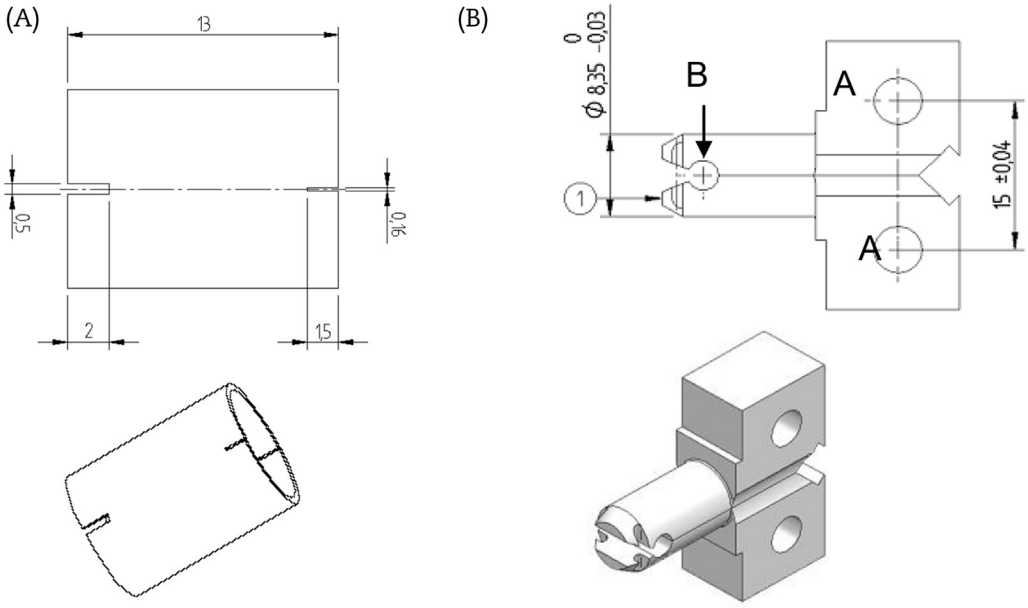

Fig. 2. Equipment used in PLT technique. Schematics of the (A) PLT specimen and (B) fixture. PLT, pin-loading tension.

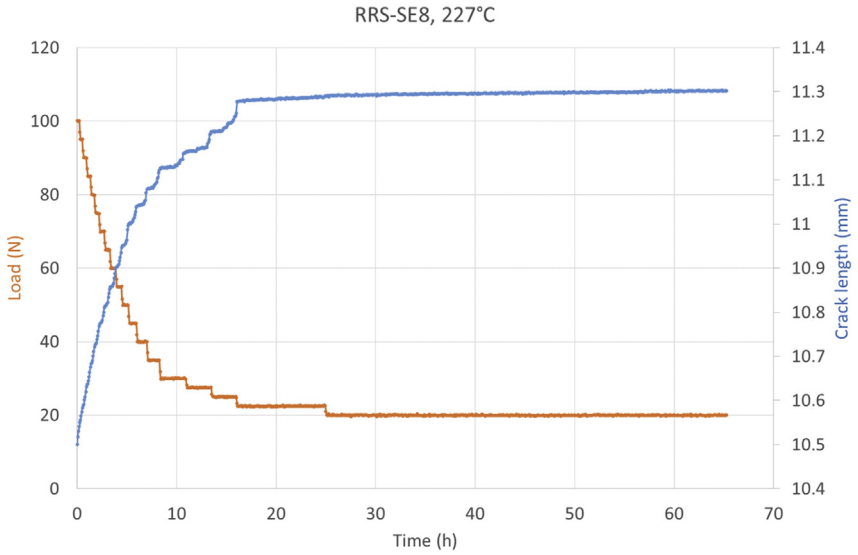

Fig. 3. Typical diagram of a PLT test where the load and crack length are plotted versus time. PLT, pin-loading tension.

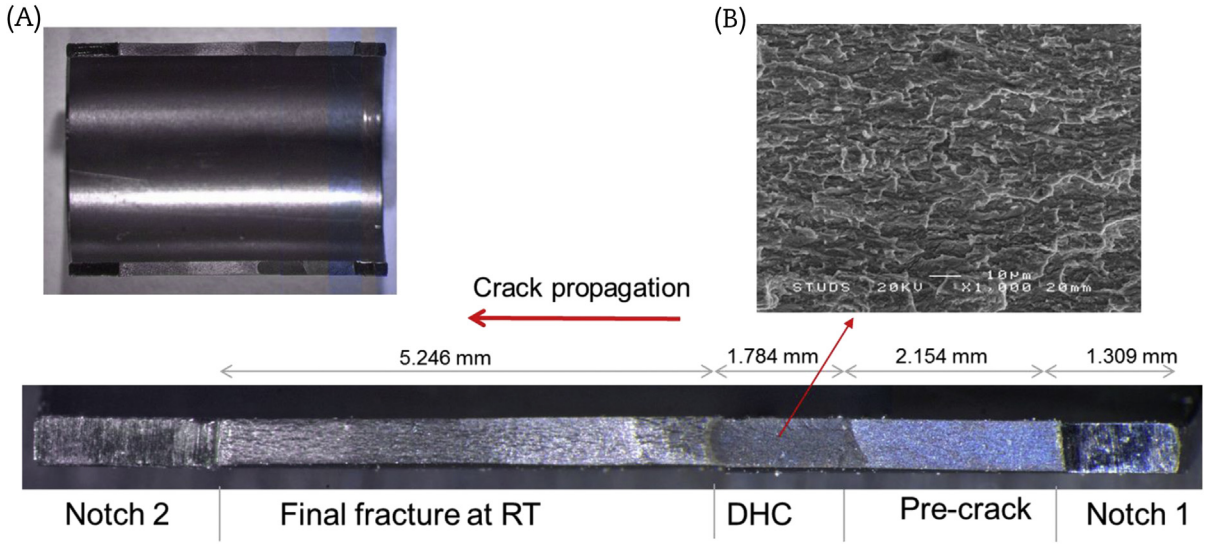

Fig. 4. Images showing fracture surfaces after the test. (A) Two parallel fracture surfaces starting at the two opposite notches in the PLT sample. (B) The DHC area in higher magnification. DHC, delayed hydride cracking; PLT, pin-loading tension.

The geometry correction factor, $f(a/W)$, was determined experimentally from compliance measurements resulting in:

$$f(a/W) = -360.99(a/W)^3 + 787.15(a/W)^2 - 468.73(a/W) + 92.203 \quad (4)$$

K_{IH} was determined by calculating K_I for the effective crack length when the crack was arrested at the final load.

In Fig. 5, K_{IH} is plotted versus the temperature. One can observe that there is moderate temperature behavior at lower temperatures. Around 300°C, there is a sharp increase in K_{IH}, indicating that the upper temperature limit for DHC was approached. The lowest value for K_{IH} was observed at 227°C and was determined to be 2.6 ± 0.3 MPa $\sqrt{m}$. Applying Eq. (1), and again applying the US Nuclear Regulatory Commission limit of 90 MPa, the critical incipient flaw depth to initiate DHC at 227°C would be 0.33 mm for an elliptic flaw and 0.22 mm for a long flaw.

4. Discussion

The observed temperature dependence of K_{IH} can be explained in terms of the effect of temperature on the yield stress of the zirconium alloy and the fracture stress of hydrides. Shi and Puls [24] observed that the hardness of the matrix relative to the hardness of the hydrides affected crack formation in single hydrides in an unirradiated Zr–2.5 Nb alloy. Single hydrides in a matrix cracked upon loading only if the yield strength of the matrix was higher than the fracture stress of the hydrides at the test temperature. Since the decrease in the fracture stress of the hydrides declined less with temperature than the decrease in yield stress with temperature, there was a temperature crossover point above which no hydrides cracked. Another explanation for the upper temperature limit of DHC is that the stresses in front of the crack tip relaxes at higher temperature by creep, which causes the crack to be blunt.

Table 3
Summary of test results.

Test Temperature	Sample ID	C_H (wppm)	Initial Load (N)	Final load (N)	a ^{notch} (mm)	a^{fatigue} (mm)	a ^{DHC} (mm)	a $^{rear\text{-}notch}$ (mm)	Sample length (mm)
250°C	RRS-pre11	≈134	120	20	1.35	1.80	1.95	1.96	12.72
					1.38	2.09	1.95	1.96	12.71
	RRS-SE1	≈134	120	20	1.43	1.62	1.76	1.98	13.0
					1.14	1.71	1.71	1.72	13.0
	RRS-SE3	≈134	100	25	1.19	1.43	1.14	1.67	12.68
					1.28	2.00	2.57	1.67	12.68
227°C	RRS-SE6	≈134	100	25	1.14	1.95	1.71	0.87	12.65
					1.19	1.48	1.24	0.81	12.57
	RRS-SE7	≈134	100	15	1.43	1.95	2.38	1.89	12.57
					1.44	1.38	1.79	1.83	12.52
	RRS-SE8	≈134	100	20	1.44	1.39	1.09	1.32	12.70
					1.50	1.42	1.41	1.31	12.63
288°C	RRS-SE9	≈134	100	40	1.32	1.48	1.10	1.84	12.74
					1.36	1.51	1.09	1.92	12.58
	RRS-SE10	≈116	100	60	1.40	1.44	0.68	1.03	12.72
					1.53	1.05	0.94	1.03	12.72
	RRS-SE11	≈116	100	50	1.34	1.56	0.84	1.71	12.71
					1.32	1.27	0.90	1.68	12.76
295°C	RRS-SE12	≈116	100	50	1.50	1.34	0.43	3.10	12.60
					1.44	1.69	0.88	3.10	12.70
315°C	RRS-SE13	≈116	100	85	1.45	1.60	0.36	1.87	12.60
					1.45	1.83	0.52	1.79	12.60

DHC, delayed hydride cracking.

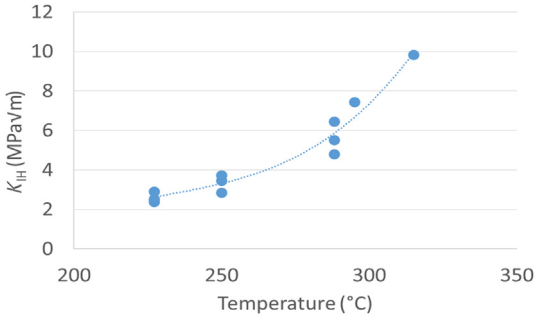

Fig. 5. Threshold stress intensity factor as a function of temperature. K_{IH}, threshold stress intensity factor.

This work was performed on unirradiated fuel cladding. Irradiated cladding exhibits irradiation hardening and thereby an increase in yield stress. This is expected to affect the K_{IH} and the upper temperature limit for DHC. On the contrary, the Zry-4 cladding material in these tests was stress relieved and therefore exhibited higher yield stress than the recrystallization annealed material, which is used in the reactor. These two effects might cancel each other out. In any case, the tests should be repeated for irradiated Zry-4 cladding to establish the effect of irradiation on K_{IH}.

Conflicts of interest

There is no conflict of interest.

Acknowledgments

The tests were a part of a coordinated research project carried out under the sponsorship of the IAEA. The authors would like to express their appreciation to the members of the CRP group for technical discussions and advice. Bo Johansson performed all the tests at Studsvik Nuclear Laboratory for mechanical testing.

References

[1] W.L. Mudge, Effect of hydrogen on the embrittlement of zirconium and zirconium-tin alloys, Symposium on zirconium and zirconium alloys, ASM, Metals Park, OH, 1953, pp. 146–167.
[2] C.E. Coleman, D. Hardie, The hydrogen embrittlement of zirconium in slow-bend tests, J. Nucl. Mater. 19 (1966) 1–8.
[3] J.B. Bai, C. Prioul, D. Francois, Hydride embrittlement in Zircaloy-4 plate: part I, influence of microstructure on the hydride embrittlement in Zircaloy-4 at 20°C and 350°C, Metall. Trans. 25A (1994) 1185–1197.
[4] D. Hardie, The influence of the matrix on the hydrogen embrittlement of zirconium in bend tests, J. Nucl. Mater. 42 (1972) 317–324.
[5] C.J. Simpson, C.E. Ells, Delayed hydrogen embrittlement of Zr-2.5wt% Nb, J. Nucl. Mater. 52 (1974) 289–295.
[6] D.O. Northwood, U. Kosasih, Hydrides and delayed hydrogen cracking in zirconium and its alloys, Int. Metals Rev. 28 (1983) 92–121.
[7] R. Dutton, K. Nuttall, M.P. Puls, L.A. Simpson, Mechanisms of hydrogen induced delayed cracking in hydride forming materials, Metall, Trans 8A (1977) 1553–1562.
[8] S. Sagat, M.P. Puls, SMiRT 17, Paper # G06–4.
[9] A. McMinn, E.C. Darby, J.S. Schofield, The terminal solid solubility of hydrogen in zirconium alloys, in: G.P. Sabol, G.D. Moan (Eds.), Twelfth International Symposium of Zirconium in the Nuclear Industry, 1354, ASTM STP, 2000, pp. 173–195.
[10] P. Vizaino, A.D. Banchik, J.P. Abriata, Solubility of hydrogen in Zircaloy-4: irradiation induced increase and thermal recovery, J. Nucl. Mater. 304 (2002) 96–106.
[11] J.J. Kearns, Terminal solubility and partitioning of hydrogen in the alpha phase of zirconium, Zircaloy-2 and Zircaloy-4, J. Nucl. Mater. 22 (1967) 292–303.
[12] V. Grigoriev, Parametric study of DHC in fuel cladding, Workshop on hydrogen induced failures, November 17, 2009. Sweden.
[13] Y.S. Kim, Delayed hydride cracking of spent fuel rods in dry storage, J. Nucl. Mater. 378 (2008) 30–34.
[14] C.E. Coleman, The CANDU experience AECL, history: cause and remedies, Workshop on hydrogen induced failures, November 17, 2009. Sweden.
[15] F.H. Huang, W.J. Mills, Delayed hydride cracking behavior for zircaloy-2 tubing, Metall. Trans. A 22A (1991) 2049–2060.
[16] Y.S. Kim, S.C. Kwon, S.S. Kim, Crack growth pattern and threshold stress intensity factor, KIH, of Zr-2.5% Nb alloy with the notch direction, J. Nucl. Mater. 280 (2000) 304–311.
[17] D. Yan, R.L. Eadie, The threshold behaviour of delayed hydride cracking in Zr-2.5wt%Nb, Int. J. Pressure Vessels Piping 77 (2000) 167–177.
[18] S.-Q. Shi, M.P. Puls, Criteria for fracture initiation at hydrides in zirconium alloys, I: sharp crack tip, J. Nucl. Mater. 208 (1994) 232–242.
[19] C.E. Coleman, J.F.R. Ambler, Susceptibility of zirconium alloys to delayed hydride cracking, in: A.L. Lowe, G.W. Parry (Eds.), Zirconium in the Nuclear Industry, 633, ASTM STP, 1977, pp. 589–607.
[20] V. Grigoriev, R. Jakobsson, Delayed hydrogen cracking velocity and J-integral measurements on irradiated BWR cladding, J. ASTM Int. 2 (8) (2005) 12434.
[21] T. Kubo, K. Sakamoto, T. Higuchi, Development of a new technique for the in-situ observation of the DHC process under a SEM to measure the crack extension rate in a radial direction of Zry-2 tubes, 2008 Water Reactor Fuel Performance Meeting, October 19–23, 2008. Soul, Korea.
[22] C.F. Tiffany, J.N. Masters, Applied fracture mechanics, in: W.F. Brown Jr. (Ed.), Fracture Toughness Testing and its Applications, ASTM STP 381, American Society for Testing and Materials, Philadelphia, PA, 1965, pp. 249–277.
[23] US Nuclear Regulatory Commission, Standard review plan for spent fuel dry storage systems at a general license facility, NUREG-1536, 2009.
[24] S.-Q. Shi, M.P. Puls, Fracture strength of hydride precipitates in Zr–2.5Nb alloys, J. Nucl. Mater. 275 (1999) 312–317.